

Role of Surface Energy Coefficient in the Fusion Reactions Induced by Halo Projectiles

Raj Kumari

Assistant Professor

Department of Physics, D. A. V. College, Sector 10, Chandigarh 160011, India

rajkumari80pu@gmail.com

ABSTRACT

Recent advancements in the radioactive-ion beams facilities around the world have enabled us to explore many new elements in the nuclear chart. Many of the nuclei predicted in the stability valley have also been confirmed experimentally. The separation energy of last nucleon decreases as we move away from line of stability and it disappears at the drip line. The quest to understand the structure of nuclei at the neutron-drip line had led to the discovery of unexpected exotic structures of halo nuclei. The study of halo nuclei provides an opportunity to examine the interaction between the neutrons in a very low density and nearly proton-free environment. In one of our earlier study, the effect of halo structure on the fusion cross sections was studied and the study revealed that the extended halo radii affect significantly the barrier heights as well as fusion probabilities. Here, we aim to study the role of surface energy coefficient in the fusion reactions induced by halo projectiles by using a proximity-based potential. Different versions of Aage Winther (AW95) potential have been used to account for different surface energy effects. The fusion reactions induced by neutron-halo (^6He) and proton-halo (^8B) projectiles have been analyzed.

Key Words: Proximity-based potential, Halo nucleus, Surface energy coefficient.

INTRODUCTION

A halo nucleus, as the name given by Hansen and Jonson [1], consists of a core and extremely weakly-bound neutrons/protons in the classically forbidden region around it. These halo neutrons/protons have maximum probability of being located at distances much larger than the usual nuclear radius and hence, have very less separation energy. The average nucleon separation energy in a stable nucleus is about 6-8 MeV, which however, in case of halo nucleus is close to 1 MeV. These exotic nuclei have a wider density distribution and narrower momentum distribution as compared to the stable nuclei. The most studied neutron-halo nuclei are ^6He , ^{11}Li and ^{11}Be due to availability of these beams with good intensity and variable energies. In addition to neutron halos, other nuclei at drip line are protons halos, which are less available due to the presence of repulsive Coulomb field. Some of the proton-halo nuclei are ^8B , ^{17}F etc. In one of our study [2], it has been shown that the major factor responsible for enhancing the fusion yield in the reactions



involving proton-halo projectiles is their extended size. However, in case of reactions involving neutron-halo projectiles, strong size effects mainly contributes in the break-up process or transfer process rather than the fusion yield. Hence, the effect of extended sizes or halo structures on the fusion probabilities in case of halo nuclei strongly depends upon the nature of the halo nuclei *i.e.* proton halo or neutron halo.

The study by Dutt and Puri [3] and later by Gharaei and Ghodsi [4] have revealed that surface energy coefficient influences the fusion barrier by significant amount. These studies showed that different values of surface energy coefficients play an important role in the fusion reactions induced by strongly as well as weakly-bound projectiles. Motivated by these studies, we have attempted to study the role of surface energy coefficient in the fusion reactions induced by neutron-halo (^6He) and proton-halo (^8B) projectiles.

METHODOLOGY

Two different approaches macroscopic as well as microscopic are available in the literature for calculating the real part of the optical potential, which is significant for describing processes like fusion/fission reactions. A macroscopic approach considers the gross properties of nuclei as done in liquid drop model. Based upon this approach, the proximity potential is the widely used potential in the nuclear collisions.

The proximity potential is based on the theorem which states that “*the force between two gently curved surfaces in close proximity is proportional to the interaction potential per unit area between two flat surfaces*” [5]. The origin of this potential is proximity force. These attractive forces come into play when two surfaces are brought in close contact (within a distance comparable with the surface thickness *i.e.* 2 - 3 fm). According to Blocki *et al.* [5], the proximity potential can be expressed as a product of simple geometrical factor and an universal function. The geometrical factor depends on the masses of the colliding nuclei, whereas universal function is independent of the features of the colliding nuclei. It, instead, depends on the separation distance (s). The proximity potential can be written as:

$$V_N^{\text{Prox. 77}}(R_P + R_T + s) = 4\pi\gamma\beta C \phi(\zeta) \text{ MeV}, \quad (1)$$

where ‘ s ’ is the distance between two surfaces. The surface energy coefficient (γ) is taken from the Lysekil mass formula, which has the form:

$$\gamma = \gamma_0 [1 - K_s I^2] \text{ MeV/fm}^2, \quad (2)$$

where ($\gamma_0 = 0.9517 \text{ MeV/fm}^2$) is the surface energy constant and $K_s (= 1.7826)$ is the surface asymmetry constant. The parameter $I (= [N-Z]/[N+Z])$ represents the neutron excess content, where N and Z being the total neutron and proton number, respectively. The parameter β in the Eq. (1) represents surface width and is taken to be close to unity. With the passage of time, many new modifications were suggested in the proximity potential [6][7].



Proximity Type Parameterized Potentials: Many authors parameterized their potentials in the proximity fashion, where nucleus-nucleus potentials were expressed as a product of geometrical factor and universal function [8][9]. One of such attempts which is widely used in the literature is Aage Winther Potential (AW 95) as discussed below:

1. AW 95: Aage Winther [8] adjusted the parameters of the nucleus-nucleus interaction potential, which was based on the Woods-Saxon parameterization, by fitting the experimental data for heavy-ion elastic scattering. For further reading, reader is referred to Ref. [7].

In the present study, different values of surface energy coefficients (γ -MN76, γ -MN95, γ -MS00 and γ -PD03) are used in the proximity based potential due to AW 95 to account for different surface energy effects. These modified versions of AW 95 are described below:

2. AW 95 (γ -MN76): This modified version utilizes the values of surface energy coefficient given by Möller and Nix [10]. Here $\gamma_0 = 1.460734 \text{ MeV/fm}^2$ and $K_s = 4.0$.

3. AW 95 (γ -MN95): Later on, values of γ_0 and K_s were refitted by using better mass formula due to Möller *et al.* [11]. This new set of values reads as $\gamma_0 = 1.25284 \text{ MeV/fm}^2$ and $K_s = 2.345$.

4. AW 95 (γ -MS00): This modified version uses the form of surface energy coefficient given by Myers and Swiatecki [12]. This form of surface energy coefficient depends upon the neutron skin of the two colliding nuclei.

5. AW 95 (γ -PD03): This modified version utilizes the surface energy coefficients given by Pomorski and Dudek [13], which also includes different curvature effects in the liquid drop model. This study provided the values of 1.08948 MeV/fm^2 and 1.9830 for coefficients γ_0 and K_s , respectively. All these values are listed in Table 1.

Table 1: The calculated values of surface energy coefficient γ (MeV/fm²) using different modified versions.

Reaction	AW 95 standard	AW 95 (γ -MN76)	AW 95 (γ -MN95)	AW 95 (γ -MS00)	AW 95 (γ -PD03)
Neutron-halo projectile					
${}^6\text{He} + {}^{209}\text{Bi}$	0.830	1.060	1.051	1.055	0.941
Proton halo projectile					
${}^8\text{B} + {}^{58}\text{Ni}$	0.965	1.511	1.278	1.108	1.108



RESULTS AND DISCUSSION

Using these different values of surface energy coefficients, the barrier heights are calculated for the reactions of ${}^6\text{He} + {}^{209}\text{Bi}$ and ${}^8\text{B} + {}^{58}\text{Ni}$ by using standard radii (AW 95) and by including halo radii extracted from the cross section measurements (AW 95^{halo}) and are listed in Table 2.

Table 2: The calculated barrier heights (in MeV) for the reactions induced by neutron- and proton-halo projectiles corresponding to different modified versions (including different values of surface energy coefficient γ). Calculations for standard radii nuclei are done by using AW 95, whereas calculations in halo nuclei case are done by using AW 95^{halo}.

Reaction	AW 95 standard V_B	AW 95 (γ -MN76) V_B	AW 95 (γ -MN95) V_B	AW 95 (γ -MS00) V_B	AW 95 (γ -PD03) V_B
Standard Radius					
${}^6\text{He} + {}^{209}\text{Bi}$	19.95	19.67	19.68	19.68	19.81
${}^8\text{B} + {}^{58}\text{Ni}$	21.10	20.41	20.66	20.88	20.88
Halo Radius					
${}^6\text{He} + {}^{209}\text{Bi}$	18.66	18.42	18.43	18.42	18.54
${}^8\text{B} + {}^{58}\text{Ni}$	20.55	19.89	20.13	20.34	20.34

From the table, we see that the fusion barrier heights are lowest for the cases with largest value of surface energy coefficient. This trend is observed in both cases *i.e.* calculations involving standard radius as well as halo radius. Also, the barrier heights corresponding to the halo radius are lower compared to those in the case of standard radius.

In Figs. 1 (a) and (b), the nuclear potentials V_N (MeV) are displayed as a function of inter nuclear distance R (fm) for the reactions of ${}^6\text{He} + {}^{209}\text{Bi}$ and ${}^8\text{B} + {}^{58}\text{Ni}$, respectively. The pink (dotted), black (dashed), navy (dash-dotted), purple (dash-double dotted) and dark cyan (solid) thin and thick lines correspond to calculations using standard radius and halo radius, respectively, in AW 95, AW 95 (γ -MN76), AW 95 (γ -MN95), AW 95 (γ -MS00) and AW 95 (γ -PD03). In Fig. 1 (a), AW 95 (with $\gamma = 0.830$) leads to shallowest nuclear potential compared to other versions and AW 95 (γ -MN76)(with $\gamma = 1.060$)/AW 95 (γ -MS00)(with $\gamma = 1.055$) give deepest nuclear potential. This is due to the reason that larger value of the surface energy coefficient corresponds to more surface tension and hence, more attraction. However, when the



halo radius deduced from the cross section measurements for ${}^6\text{He}$ is included in the calculations *i.e.* AW 95^{halo}, the nuclear potentials corresponding to different versions of surface energy coefficients are significantly lowered. This is due to the fact that halo radius of ${}^6\text{He}$ nucleus

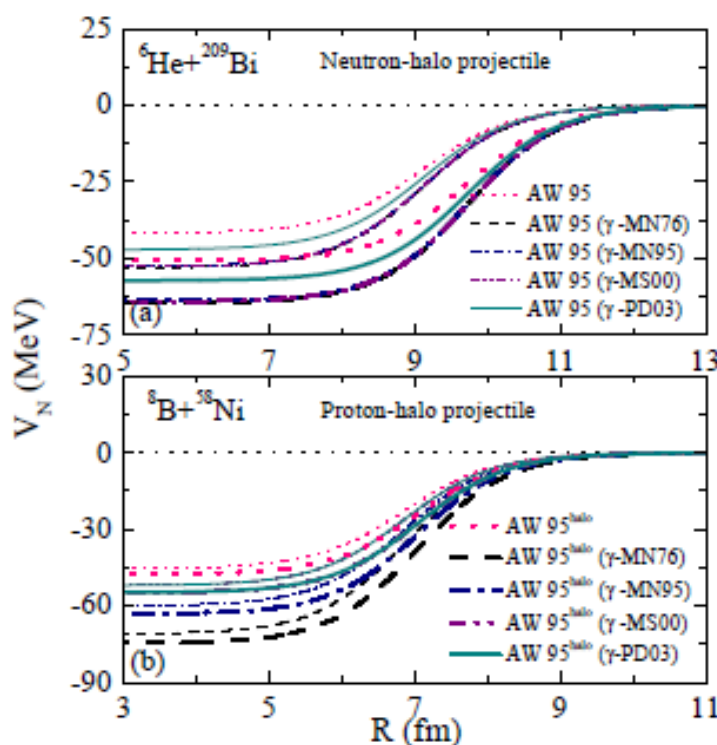


Figure 1: The nuclear potential V_N (MeV) is displayed as a function of internuclear distance R (fm) for the reactions of ${}^6\text{He} + {}^{209}\text{Bi}$ and ${}^8\text{B} + {}^{58}\text{Ni}$. Various symbols are explained in the text.

(*i.e.* 2.71 fm, deduced from measurements [14]) is large compared to its standard radius (*i.e.* 2.09 fm, calculated using AW 95). Due to large halo radius, the nuclear forces start acting even at larger distances and hence, resulting in deeper nuclear potential. Therefore, we find that largest value of surface energy coefficient and inclusion of halo radius lead to deepest nuclear potential and hence, lowest barrier height for the reaction of ${}^6\text{He} + {}^{209}\text{Bi}$. Similar study is also conducted for the fusion reaction of ${}^8\text{B} + {}^{58}\text{Ni}$ involving proton-halo projectile (shown in Fig. 1 (b)). The observed trends are similar to that in earlier case, but, the changes observed in the depth of nuclear potential in this case is less. This is because, the surface energy coefficient also depends upon the asymmetry parameter (I), which is zero in case of ${}^8\text{B} + {}^{58}\text{Ni}$ and is non-zero (*i.e.* 0.21) in the case of ${}^6\text{He} + {}^{209}\text{Bi}$. Moreover, the difference between the halo radius of ${}^8\text{B}$ nucleus (*i.e.* 2.50 fm, deduced from measurements [14]) and its standard radius (*i.e.* 2.31 fm, calculated using AW 95) is less compared to that in ${}^6\text{He}$ case.

In Figs. 2 (a) and (b), the reduced fusion cross sections σ_{reduced} (mb) are displayed as a function of reduced center of mass energy, E_{reduced} (MeV) for the reactions of ${}^6\text{He} + {}^{209}\text{Bi}$ and ${}^8\text{B} + {}^{58}\text{Ni}$, respectively. We notice higher fusion cross sections corresponding to higher values of γ and these values are comparatively higher for the halo case. This is because, halo radius and largest value of γ give deepest nuclear potential and hence lowest Coulomb barrier. This results in



enhanced fusion cross sections and a close agreement with experimental data in case of ${}^8\text{B} + {}^{58}\text{Ni}$ reaction.

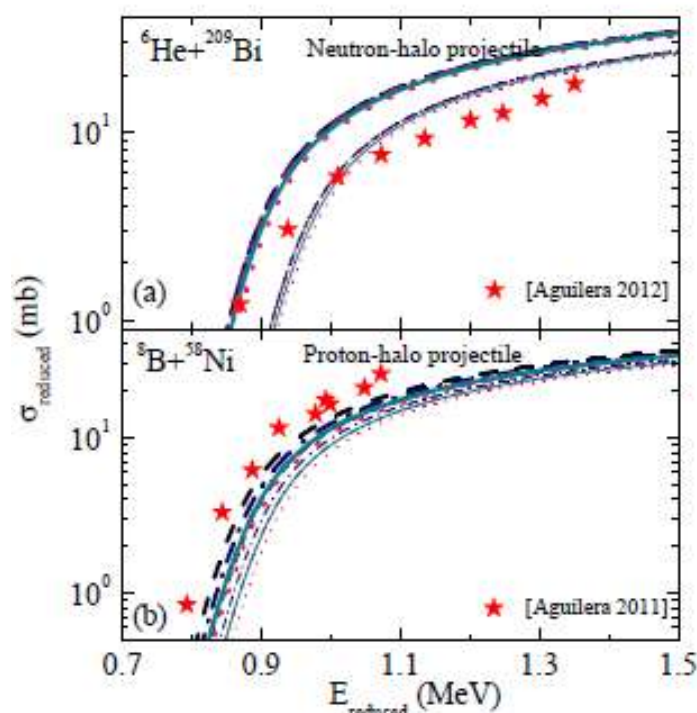


Figure 2: The reduced fusion cross-sections for the reactions of ${}^6\text{He} + {}^{209}\text{Bi}$ and ${}^8\text{B} + {}^{58}\text{Ni}$ as a function of reduced center of mass energies. The experimental data is taken from Aguilera 2012 [15] and Aguilera 2011 [16]. Various lines have the same meaning as in Fig. 1.

This study reveals that surface energy coefficient plays a significant role in the fusion reactions induced by the halo projectiles.

SUMMARY

We investigated the role of surface energy coefficient in the fusion reactions induced by the halo projectiles by employing different modified versions of Aage Winther (AW 95) potential. From this study, we concluded that larger value of surface energy coefficient leads to deeper nuclear potential and enhanced fusion cross sections at all incident energies.

REFERENCES

- [1] Hansen P. G. and Jonson B., “The Neutron Halo of Extremely Neutron-Rich Nuclei”, *Europhysics Letters*, Vol. 4, p. 409-414, August 1987.
- [2] Kumari R., “Study of Fusion Probabilities with Halo Nuclei using Different Proximity based Potentials”, *Nuclear Physics A*, Vol. 917, p. 85-91, November 2013.



- [3] Dutt I. and Puri R. K., "Role of Surface Energy Coefficients and Nuclear Surface Diffuseness in the Fusion of Heavy-ions", *Physical Review C*, Vol. 81, Issue 047601, April 2010.
- [4] Gharaei R. and Ghodsi O. N., "Role of Surface Energy Coefficients and Temperature in the Fusion Reactions Induced by Weakly Bound Projectiles", *Commun. Theoretical Physics*, Vol. 64, p. 185-196, August 2015.
- [5] Blocki J., Randrup J., Swiatecki J. and Tsang C. F., "Proximity Forces", *Annals of Physics*, Vol. 105, p. 427-462, June 1977.
- [6] Dutt I. and Puri R. K., "Systematic Study of the Fusion Barriers using Different Proximity-type Potentials for N=Z Colliding Nuclei: New Extensions", *Physical Review C*, Vol. 81, Issue 044615, April 2010.
- [7] Dutt I. and Puri R. K., "Comparison of Different Proximity Potentials for Asymmetric Colliding Nuclei", *Physical Review C*, Vol. 81, Issue 064609, June 2010.
- [8] Winther A., "Dissipation, Polarization and Fluctuation in Grazing Heavy-ion Collisions and the Boundary to the Chaotic Regime", *Nuclear Physics A*, Vol. 594, p. 203-245, February 1995.
- [9] Denisov V. Y., "Interaction Potential between Heavy Ions", *Physics Letters B*, Vol. 526, p. 315-321, February 2002.
- [10] Möller P. and Nix J. R., "Macroscopic Potential-energy Surfaces for Symmetric Fission and Heavy-ion reactions", *Nuclear Physics A*, Vol. 272, p. 502-532, November 1976.
- [11] Möller P., Nix J. R., Myers W. D. and Swiatecki W. J., "Nuclear Ground-State Masses and Deformations", *Atomic Data and Nuclear Data Tables*, Vol. 59, p. 185-381, March 1995.
- [12] Myers W. D. and Swiatecki W. J., "Nucleus-nucleus Proximity Potential and Superheavy Nuclei", *Physical Review C*, Vol. 62, Issue 044610, September 2000.
- [13] Pomorski K. and Dudek J., "Nuclear Liquid-drop Model and Surface-curvature Effects", *Physical Review C*, Vol. 67, Issue 044316, April 2003.
- [14] Al-Khalili J. S., Tostevin J. A. and Thompson I. J., "Radii of Halo Nuclei from Cross Section Measurements", *Physical Review C*, Vol. 54, Issue 1843, October 1996.
- [15] Aguilera E. F. and Kolata J. J., "Angular Momentum Limit for Fusion of Halo and Weakly Bound Systems", *Physical Review C*, Vol. 85, Issue 014603, January 2012.
- [16] E. F. Aguilera, "Near-Barrier Fusion of the $^8\text{B}+^{58}\text{Ni}$ Proton-Halo System", *Physical Review Letters*, Vol. 107, Issue 092701, August 2011.

